Two-photon absorption properties of fluorescent proteins

Mikhail Drobizhev[1], Nikolay S Makarov[1,4], Shane E Tillo[2,4], Thomas E Hughes[2] & Aleksander Rebane[1,3]

Two-photon excitation of fluorescent proteins is an attractive approach for imaging living systems. Today researchers are eager to know which proteins are the brightest and what the best excitation wavelengths are. Here we review the two-photon absorption properties of a wide variety of fluorescent proteins, including new far-red variants, to produce a comprehensive guide to choosing the right fluorescent protein and excitation wavelength for two-photon applications.

Two-photon laser scanning microscopy (2PLSM)[1,2] of cells and tissues expressing fluorescent proteins is becoming a powerful tool for biological studies at different levels of organization[2–4]. The advantages of two-photon excitation include reduced out-of-focus photobleaching, less autofluorescence, deeper tissue penetration and intrinsically high three-dimensional resolution[1,2]. The 2PLSM approach should make it possible to obtain even better optical recordings of ion concentration and cell signaling with genetically targeted sensors[5,6]. Two-photon excitation of fluorescent proteins can also be considered as potentially advantageous in the contexts of genetically targeted deep photodynamic therapy or chromophore-assisted light inactivation[6], three-dimensional optical memory[7] as well as super-resolution (subdiffraction–limited) imaging techniques such as stimulated emission depletion[8], photoactivated localization microscopy and stochastic optical reconstruction microscopy[9].

To fully realize the potential of two-photon excitation of the fluorescent proteins, it is important to know their two-photon absorption (2PA) spectra, cross-section values, σ_2, and two-photon excitation action cross-section (brightness) values, $\sigma_2' = \sigma_2 \times \varphi$, in which φ is the fluorescence quantum yield. The linear, one-photon absorption (1PA) spectra and extinction coefficients of many fluorescent proteins have been described and reviewed previously[5,6,10] (**Supplementary Table 1**), but the 1PA properties are not sufficient to predict the key 2PA properties such as optimum excitation wavelength and maximum brightness (**Boxes 1** and **2**).

Here we present the results of a systematic characterization of the 2PA properties of 48 fluorescent proteins, combining published data on some blue (enhanced (E)BFP series), cyan (ECFP and monomeric (m)Cerulean), teal (mTFP series), green (EGFP, mWasabi and mAmetrine), orange and red (DsRed, mRFP and 'Fruit' series) fluorescent proteins[11,12] with new data on the most promising far-red variants, such as mRaspberry, E2-Crimson, mKate, mKate2, tandem dimer (td)Katushka2, mGrape3, mNeptune, eqFP650 and eqFP670. The 2PA spectrum (presented in absolute cross-section values per mature chromophore) represents the fundamental molecular property of a fluorescent protein, a property that could strongly constrain its utility in any two-photon application. The data presented here are an important first step in determining which proteins are brightest upon two-photon excitation and at what wavelengths, but there are other factors—such as expression rate, photostability, photoswitching efficiency or ability to generate singlet oxygen—that also need to be considered when selecting the right mutant for a particular two-photon application.

[1]Department of Physics, Montana State University, Bozeman, Montana, USA. [2]Department of Cell Biology and Neuroscience, Montana State University, Bozeman, Montana, USA. [3]National Institute of Chemical Physics and Biophysics, Akadeemia tee, Tallinn, Estonia. [4]Present addresses: School of Chemistry and Biochemistry, Georgia Institute of Technology, Atlanta, Georgia, USA (N.S.M.) and Vollum Institute, Oregon Health and Science University, Portland, Oregon, USA (S.E.T.). Correspondence should be addressed to M.D. (drobizhev@physics.montana.edu).

PUBLISHED ONLINE 28 APRIL 2011; DOI:10.1038/NMETH.1596

BOX 1 GLOSSARY OF TERMS

Electronic transitions. Absorption and fluorescence emission of photons by a fluorescent protein are due to the system of π-conjugated electrons of the chromophore. The change of its electronic state, associated with absorption or emission, is called electronic transition. The process corresponding to absorption of a photon involves a transition of the electronic system from the lowest-energy ground state (S_0) to an electronically excited higher-energy state (S_n, in which n = 1, 2 and so on). The higher the energy of the final state, the shorter the wavelength of the corresponding photon is. Spontaneous transition from the first excited state (S_1) back to the ground state (S_0) with simultaneous emission of a photon is called fluorescence.

Vavilov-Kasha's rule. According to Vavilov-Kasha's rule, the fluorescence of polyatomic molecules always occurs from the lowest excited state (S_1), independent of which state (S_1, S_2, S_3 and so on) was initially excited. This is because the non-radiative relaxation from the higher energy levels (S_2, S_3 and so on) to the S_1 level proceeds very quickly, on the picosecond time scale, compared to the nanosecond lifetime of the S_1 level. As this fast relaxation is nonradiative, it does not depend on the mode of excitation, that is, one- or two-photon.

Vibronic transitions. The vibrational state of a molecule, related to the movement of its nuclei, can also change upon electronic transition. Such a transition is called a vibronic transition, in contrast to the pure electronic one, where only the electronic state is changed. In the ground electronic state, a molecule usually occupies the lowest possible vibrational state because its typical vibrational quanta are much larger than the thermal energy. If the excitation photon frequency is larger than the frequency of the pure electronic transition, the higher vibrational levels of an excited electronic state can be reached, leading to a vibronic transition in absorption. In contrast, the fluorescence photons can have lower energy than the pure electronic transition energy because the transitions starting from the lowest vibrational level of the S_1 electronic state can terminate at the vibrationally excited S_0 electronic state, resulting in a vibronic transition in fluorescence.

We acquired all the data using the same experimental setup, common 2PA reference standards and an all-optical method for measuring mature chromophore concentration[11] (**Supplementary Methods**). Briefly, we used a relative fluorescence method with femtosecond excitation and coumarin 485, coumarin 540A, rhodamine 610, fluorescein and styryl 9M as 2PA standards[13], which eliminated the necessity to calibrate the laser parameters. The power dependence of the fluorescence signal was quadratic for all data presented, assuring that the spectra represent pure 2PA. We collected the spectra in a much broader range (550–1,400 nm) than commonly reported, which revealed new optimal wavelengths for excitation and provided insights into the relation of 2PA properties with protein structure.

Two-photon versus one-photon absorption properties

There are several different classes of fluorescent proteins that are usually grouped according to their chromophore structure. These classes vary tremendously in terms of their absorption and fluorescence properties. Similarly, we observed large variations in the 2PA spectra of these classes (**Fig. 1** and **Supplementary Fig. 1**). Because the chromophore in fluorescent proteins is not centrosymmetric, the parity selection rules for one- and two-photon transitions are relaxed[14]. As a result, the same bands should appear in both one- and two-photon absorption spectra, although with different relative intensities. An overlap between 1PA and 2PA spectra is generally apparent for the longest-wavelength absorption band, corresponding to the first electronic transition from the ground state (S_0) to the first excited state (S_1) (**Box 2** and **Fig. 2**). For the neutral chromophores found in EBFP2.0, mAmetrine, ECFP and mBlueberry1, the corresponding 1PA and 2PA peaks coincide rather well. In the anionic chromophores of EGFP, Citrine, mOrange, DsRed2 and TagRFP, however, there is a distinct blue shift of the 2PA band relative to the 1PA band. This observation,

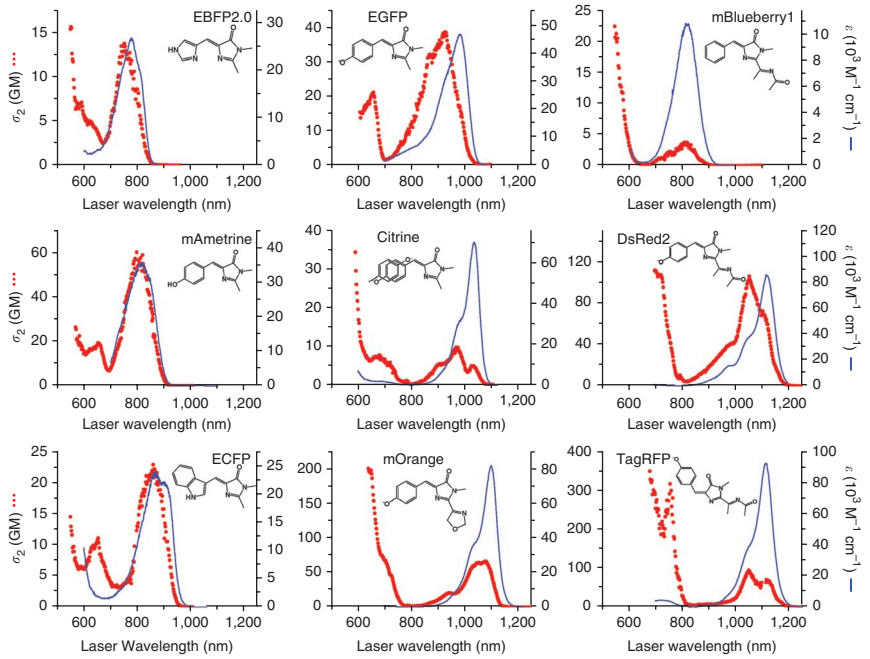

Figure 1 | One- and two-photon absorption spectra of fluorescent proteins with different chromophores. Two-photon absorption spectra (σ_2) are presented versus laser wavelength, used for excitation. For the purpose of comparison, in one-photon absorption spectra (ε) the actual excitation wavelength is multiplied by a factor of two. All spectra are presented in absolute values determined per mature chromophore. Data are reproduced in part from ref. 11. Copyright 2009 American Chemical Society.

BOX 2 ANATOMY OF TWO-PHOTON ABSORPTION SPECTRUM

Two-photon absorption cross-section, σ_2, (measured in Goeppert-Mayer units, 1 GM = 10^{-50} cm^4 s) characterizes the probability of the simultaneous absorption of two photons whose energies add up to match the molecular transition energy. Two-photon absorption (2PA) is governed by different quantum-mechanical rules than one-photon absorption (1PA), and, as a result, the 2PA spectra are often much different in shape than their one-photon counterparts, as exemplified in **Figure 2** for TagRFP. The 1PA (extinction) spectrum in the region of the S_0 to S_1 transition is described by

$$\varepsilon(\nu) = A\,|\boldsymbol{\mu}_{10}|^2 g_1(\nu) \quad (1)$$

in which A is a constant, ν is the frequency, $\boldsymbol{\mu}_{10}$ is the matrix element of the electronic transition dipole moment between states S_0 and S_1, and $g_1(\nu)$ is the 1PA line-shape function, which includes the distribution of intensity owing to vibronic transitions. The 2PA spectrum in the same region is represented, within the two-level approximation, by

$$\sigma_2(\nu) = B|\Delta\boldsymbol{\mu}_{10}|^2\,|\boldsymbol{\mu}_{10}|^2\, g_2(\nu) \quad (2)$$

in which B is another constant, $\Delta\boldsymbol{\mu}_{10}$ is the difference between permanent dipole moments of the excited (S_1) and ground (S_0) states, and $g_2(\nu)$ is the 2PA line-shape function. The shape of the 2PA spectrum, $g_2(\nu)$, is different from the shape of the 1PA spectrum, $g_1(\nu)$, because some vibronic transitions become enhanced in the two-photon process, whereas the pure electronic transition is the strongest in the one-photon process. In the S_0 to S_n transition region (**Fig. 2**), the 2PA is surprisingly strong. The 1PA in this region is described by

$$\varepsilon(\nu) = A|\boldsymbol{\mu}_{n0}|^2 g_1'(\nu) \quad (3)$$

in which $g_1'(\nu)$ is the 1PA line-shape function for this higher transition, and $\boldsymbol{\mu}_{n0}$ is the transition dipole moment connecting states S_0 and S_n. The 1PA is very weak (**Fig. 2**) because of small absolute value of $\boldsymbol{\mu}_{n0}$. The 2PA, in the three-level approximation[14], reads

$$\sigma_2(\nu) = B\nu_L^2|\boldsymbol{\mu}_{n1}|^2|\boldsymbol{\mu}_{10}|^2 g_2'(\nu)/(\nu_{10} - \nu_L)^2 \quad (4)$$

in which $\boldsymbol{\mu}_{n1}$ is the transition dipole moment between states S_1 and S_n, $g_2'(\nu)$ is the 2PA line-shape function, ν_{10} is the (peak) frequency of the S_0 to S_1 transition and ν_L is the laser frequency ($\nu_L = \nu/2$). The 2PA becomes very strong in this region because of large absolute values of $\boldsymbol{\mu}_{10}$, $\boldsymbol{\mu}_{n1}$, and quantum-mechanical effect known as resonant enhancement[14]. Resonant enhancement occurs when the laser frequency, ν_L, approaches from below the energy of the lowest S_1 state, ν_{10}, resulting in fast reduction of denominator in equation (4).

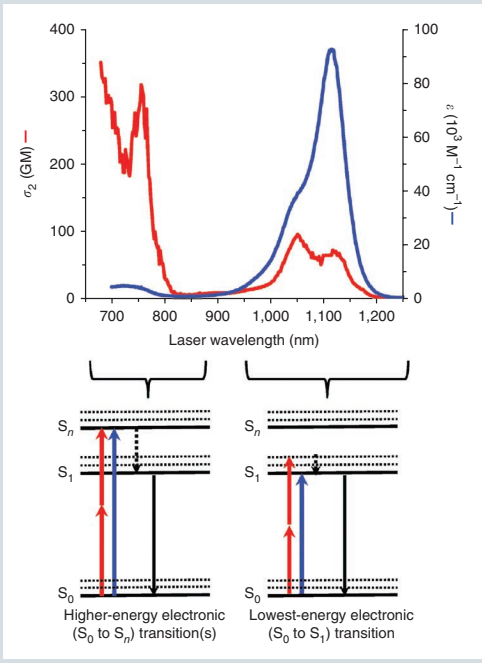

Figure 2 | Structure of the two-photon absorption spectrum of a fluorescent protein. One-photon absorption and two-photon absorption spectra of TagRFP (top). Jablonski diagram of 1PA and 2PA transitions (bottom).

previously ascribed to an enhancement of certain vibronic transitions in 2PA spectrum[11,15], illustrates why the optimal 2PA excitation wavelength cannot in general be deduced from the 1PA peak wavelength.

The most notable difference between the 2PA and 1PA spectra is the appearance of strong two-photon absorption in the region of wavelengths much shorter than those of the S_0 to S_1 transition, where 1PA is extremely weak. This recently observed 2PA feature of fluorescent proteins[14] is a consequence of higher electronic S_0 to S_n transitions, which had been predicted theoretically for various types of chromophores[16] (**Supplementary Fig. 2**). The S_0 to S_n shorter-wavelength 2PA transitions can be very intense owing to the resonance enhancement effect[14] (**Box 2**). Indeed, in some chromophores, including those of Citrine, mOrange, mBlueberry1, DsRed2 and TagRFP, this enhancement is so strong that we found optimal excitation at wavelengths much shorter than what one would expect based on the 1PA properties alone (**Fig. 1**). In the spectra of red and far-red proteins, these S_0 to S_n transitions occur at 700–770 nm, matching well with the tuning range of femtosecond Ti:sapphire lasers and thus offering new opportunities with already existing commercial 2PLSM systems[12,17]. For example, excitation of the higher S_0 to S_n transition of TagRFP simultaneously with the first, S_0 to S_1, transition of mKalama1 makes dual-color two-photon imaging possible with a single excitation laser wavelength[12]. Alternatively, two proteins with very different Stokes shifts can be used for this purpose[18].

Compared to a regular dye in solution, the chromophore of a fluorescent protein is buried in a complex, spatially organized protein environment that influences the optical properties of the chromophore through electrostatic interactions[19]. Recently, it has been shown that different hues in mutants that contain the same (DsRed-type) chromophore are caused by variations in the local electric field inside the beta barrel[20]. The shifts of the 1PA peak wavelength are accompanied by only small changes in the

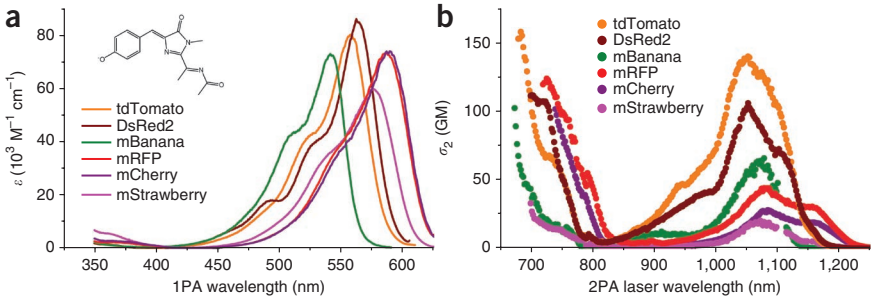

Figure 3 | One-photon absorption of the 'Fruit' proteins does not predict which is the brightest two-photon probe. (**a**,**b**) The 1PA (**a**) and 2PA (**b**) spectra of the Fruit series of fluorescent proteins. Adopted from ref. 11. Copyright 2009 American Chemical Society.

extinction coefficient (**Fig. 3a**). The local electrostatic environment also influences the 2PA properties but with the important difference that the shift of the peak absorbance is accompanied by large changes in 2PA cross-section (**Fig. 3b**). This is because the 2PA cross-section is much more sensitive to the local electric-field variations (**Box 3** and **Fig. 4**). For example, we found that Citrine was as bright as EGFP upon one-photon excitation, but much dimmer than EGFP upon two-photon excitation. This effect could be due to the change of the local field at the chromophore site caused by the high polarizability of a nearby stacking residue, Tyr203 (ref. 21).

Choosing the protein and laser for two-photon excitation

In **Table 1** we summarize the most relevant 2PA properties of representative fluorescent proteins (see **Supplementary Table 2** for all the proteins studied). Comparison of the data revealed a remarkable variability: the maximum σ_2 and brightness σ_2' changed over two orders of magnitude (**Fig. 1** and **Table 1**). These are much larger differences than those observed for one-photon extinction (ε), which changes at most by eightfold (from 10,800 M^{-1} cm^{-1} (mBlueberry1) to 85,600 M^{-1} cm^{-1} (DsRed2)). This means that identifying the right fluorescent protein for a particular 2PA application is crucial for success.

If we concentrate only on two-photon brightness, several proteins stand out as good potential two-photon probes in the Ti:sapphire tuning range. Among the proteins fluorescing in the blue-green region, the members of mTFP series were twice as bright as EGFP when excited at 870–920 nm. In the yellow-orange region of fluorescence, mOrange could be efficiently excited near

BOX 3 SENSITIVITY OF TWO-PHOTON ABSORPTION TO LOCAL ELECTRIC FIELD

Because two-photon absorption (2PA) is governed by different quantum mechanical rules, it reveals different aspects of the chromophore structure and chromophore-protein interactions. Unlike linear extinction, ε, which depends only on the transition dipole moment squared, $|\boldsymbol{\mu}_{10}|^2$, 2PA cross-section σ_2 is proportional to both $|\boldsymbol{\mu}_{10}|^2$ and $|\Delta\boldsymbol{\mu}_{10}|^2$ (compare equation (2) in **Box 2**). The consequence of this is that σ_2 is sensitive to the electric field present in the protein barrel. Therefore, σ_2 can be manipulated by changing the electrostatic environment of the chromophore. For example, in the 'Fruit' proteins, all of which have the same chromophore but different environment, the one-photon absorption (1PA) extinction coefficient varies only very slightly but 2PA cross-section increases very fast when $|\Delta\boldsymbol{\mu}_{10}|$ increases (**Fig. 4**).

The chromophore of a fluorescent protein has a permanent dipole moment in both the ground ($\boldsymbol{\mu}_0$) and excited ($\boldsymbol{\mu}_1$) states. Because of the high mobility of the π-electronic cloud, the S_0 to S_1 transition has a certain charge-transfer character, resulting in a difference between permanent dipoles ($\Delta\boldsymbol{\mu}_{10} = \boldsymbol{\mu}_1 - \boldsymbol{\mu}_0 \neq 0$). Another important property of the labile π-electron system of the chromophore is that the charge density easily redistributes upon application of external electric field **E**, thus resulting in an additional induced component of the dipole moment $\boldsymbol{\mu}^{ind}$. This induced portion of the dipole is related to the electric field through polarizability coefficient (more generally, tensor) $\boldsymbol{\alpha}$: $\boldsymbol{\mu}^{ind} = \boldsymbol{\alpha}\,\mathbf{E}$. If the polarizabilities in the ground ($\boldsymbol{\alpha}_0$) and excited ($\boldsymbol{\alpha}_1$) states are different, the change of induced dipole moment $\Delta\boldsymbol{\mu}^{ind}{}_{10}$ will contribute to the total change of dipole moment: $\Delta\boldsymbol{\mu}_{10} = \Delta\boldsymbol{\mu}^0{}_{10} + 0.5\,\Delta\boldsymbol{\mu}^{ind}{}_{10} = \Delta\boldsymbol{\mu}^0{}_{10} + 0.5(\boldsymbol{\alpha}_1 - \boldsymbol{\alpha}_0)\,\mathbf{E}$,

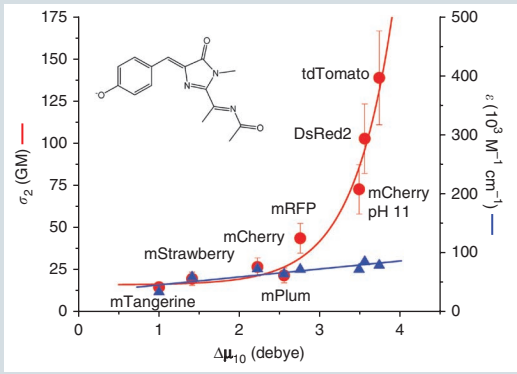

Figure 4 | Two-photon absorption is highly sensitive to the electric field in the protein environment. Dependence of the 2PA peak cross-section and the 1PA peak extinction on the change of permanent dipole moment of chromophore upon excitation, $|\Delta\boldsymbol{\mu}_{10}|$ in the 'Fruit' protein series. $|\Delta\boldsymbol{\mu}_{10}|$ is a metric of electric field intensity. Error bars, s.d.

in which index 0 in $\Delta\boldsymbol{\mu}^0{}_{10}$ corresponds to 'zero field' situation. This dependence makes $\Delta\boldsymbol{\mu}_{10}$ sensitive to the electric field. This mechanistic picture of how the chromophore electronic structure is tuned by its environment makes strong predictions for creating better fluorescent proteins for two-photon applications: one can obtain a strong gain in peak 2PA cross-section upon increasing of $|\Delta\boldsymbol{\mu}_{10}|$ (which follows the changes of **E**, or, more accurately, projection of **E** on $\Delta\boldsymbol{\mu}_{10}$). In fluorescent proteins, **E** can be altered by changing certain charged amino acids, or the hydrogen bonding network, on the axis of the chromophore dipole.

Table 1 | 2PA properties of representative fluorescent proteins

	S_0 to S_n transition			S_0 to S_1 transition		
Protein	λ_{2PA} (nm)	σ_2 (GM)	σ_2' (GM)	λ_{2PA} (nm)	σ_2 (GM)	σ_2' (GM)
EBFP2.0 (ref. 40)	552	16	11	750	13	9.2
ECFP (Clontech)	550	15	7.8	857	23	12
Cerulean[41]	550	27	16	858	23	13
mTFP1.0 (ref. 42)	667	6.4	5.4	875	70	59
EGFP (Clontech)	660	22	17	927	39	30
mAmetrine[43]	655	19	13	809	56	40
Citrine[44]	590	34	23	968	10	6.7
mKok[45]	686	93	67	1,044	41	30
mOrange[31]	640	200	140	1,080	67	47
TagRFP[46]	759	300	130	1,050	95	42
tdTomato[31]	684	316	228	1,050	278	200
DsRed2 (ref. 47)	700	112	79	1,050	103	73
mCherry[31]	740	101	24	1,080	27	6.4
mRaspberry[48]	704	346	65	1,118	31	5.8
mPlum[48]	724	114	15	1,105	22	2.9
tdKatushka2 (ref. 49)	710	645	285	1,100	143	63
mKate2 (ref. 49)	712	216	91	1,140	72	30
mNeptune[50]	750	335	57	1,105	70	12

Two-photon absorption cross-section (σ_2), two-photon brightness (σ_2'), both per mature protein are presented in two spectral regions, corresponding to the S_0 to S_n and S_0 to S_1 transitions. To obtain σ_2 and σ_2' per chromophore in the case of dimers, one has to take one-half of the corresponding values presented in the table. λ_{2PA}, laser wavelength.

730 nm, whereas TagRFP, tdTomato, DsRed, mKate, mKate2, mKate S158A, mKate S158C, tdKatushka2 and mNeptune show quite bright red fluorescence when excited at 730–770 nm.

Several proteins offer useful 2PA properties beyond the common range of Ti:sapphire lasers. In particular, those with orange to far-red fluorescence can be excited efficiently at wavelengths between 1,000 nm and 1,200 nm, where there is relatively little tissue or water absorption, weak tissue scattering and vanishingly small amounts of tissue autofluorescence[1] (**Fig. 5**). There is a good match between the 2PA peak of tdTomato and tdKatushka2 and minimum attenuation of the tissue in the spectral range from 1,000 nm to 1,150 nm. Although tdKatushka2 is not as bright as tdTomato, its fluorescence spectrum is red-shifted with respect to that of tdTomato (**Fig. 5**), fitting better to the highest transparency range. Although the region of 1,000–1,150 nm is inaccessible to standard Ti:sapphire lasers, there are other laser solutions currently available such as femto- and picosecond neodymium (Nd)- and ytterbium (Yb)-doped fiber and glass lasers.

Why do published cross-sections vary so much?

An accurate measurement of the absolute 2PA cross-section remains a technically demanding task that requires careful independent experimental evaluation of several parameters, each of which has a particular experimental error that contributes to uncertainty in the cross-section value. In pioneering work, researchers from the Webb[1,2,22,23], Schmidt[15] and Kleinfeld[3] groups reported the two-photon excitation action cross-section spectra of ECFP, EGFP, EYFP and DsRed, measured within the typical spectral range of a Ti:sapphire laser. More two-photon excitation[4,11,12,14,18,24–26] and 2PA[27] spectra followed, but the absolute two-photon excitation cross-sections obtained even for the same protein varied dramatically. For example, the peak σ_2' value of 30 Goeppert-Mayer units (GM) that we obtained for EGFP has been reported to be 1.5 GM (ref. 27), 20 GM (ref. 24), 40 GM (ref. 15), 60 GM (ref. 22), 180 GM (ref. 18) and 180 GM (ref. 2), and for mEGFP a value 300 GM has been reported[26]. Such discrepancies may be attributed to several potential sources of experimental error. First, measurements based on two-photon excited fluorescence such as the measurements we performed are usually more accurate than the nonlinear transmission techniques (including Z-scan, pump-probe and others) that have been used in some other studies[27] because the former rely on zero-background detection and require much less excitation power and lower concentration of chromophores. The high excitation used in nonlinear transmission techniques can initiate other spurious nonlinear optical processes such as 'thermal lensing', stimulated emission and scattering, resulting in underestimated 2PA cross-sections[28].

Most of the authors obtained the cross-section values by using two-photon excitation fluorescence in combination with 2PA standards. In several studies, these measurements had been performed relative to fluorescein or rhodamine B, but the actual values for these reference dyes vary in the literature[13,29]. This can explain the difference between the EGFP peak cross-section we obtained, $\sigma_2' = 30$ GM, using the fluorescein value of $\sigma_2 = 16$ GM ± 2 GM at 920 nm[13], and $\sigma_2' = 41$ GM reported by Blab *et al.*[15] that was based on a higher value ($\sigma_2 = 26$ GM ± 8 GM) for fluorescein at the same wavelength[29].

Finally, most measurements have been complicated by an uncertainty over the actual concentration of the mature chromophore in a protein sample. Typically the concentration is measured using the bicinchoninic acid (BCA) protein assay or alkaline denaturation methods. Both can introduce errors, especially if the protein folds or matures poorly and/or the chromophore is unstable under alkaline denaturating conditions[30]. This can be circumvented by using an all-optical approach[11] that relates the fluorescence lifetime and quantum yield to the extinction

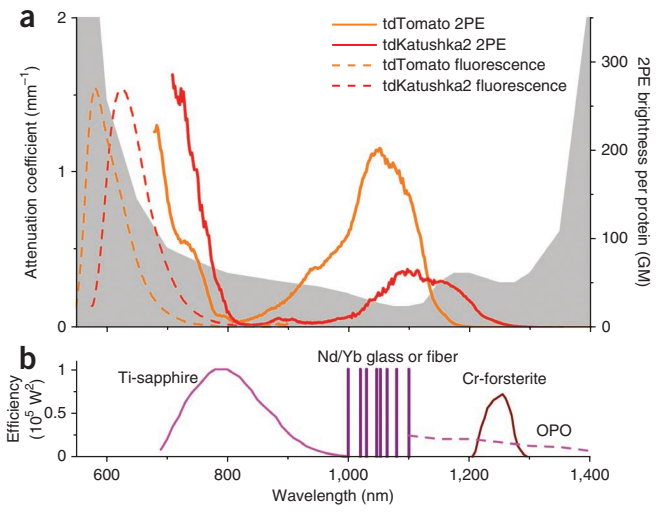

Figure 5 | Matching of two-photon excitation spectra of red fluorescent proteins with the optimum tissue transparency and with the wavelengths of some short-pulse laser systems. (**a**) Typical tissue transparency window[39] (gray) presented as attenuation coefficient (left *y* axis), two-photon excitation (2PE) brightness spectra per protein chain of tdTomato and tdKatushka2, (right *y* axis), and their corresponding normalized fluorescence spectra. (**b**) Effective laser efficiency relevant to two-photon excitation (average power squared divided by repetition rate and pulse duration) of several commercial femtosecond lasers.

coefficient (**Supplementary Methods** and **Supplementary Fig. 3**). Comparison of our measurements of mBanana[11] and those reported previously[31] revealed that this protein has an order of magnitude higher extinction coefficient than previously thought because it appears that only a small portion of the protein matures to form the chromophore.

Although the last 15 years of work have produced a remarkably wide range of reported cross-section values for EGFP and other commonly used proteins, there is an emerging consensus for some of the proteins. The cross-section of EGFP at 850 nm recently obtained by Herz *et al.*[4] is in perfect agreement with our result at the same wavelength, and recent data by Hashimoto *et al.*[24] on EGFP, BFP and ECFP are also consistent with our measurements (**Supplementary Table 2**).

Remaining challenges

A great deal of effort has been devoted to optimizing one-photon properties of fluorescent proteins, but surprisingly little attention has been paid to creating brighter mutants for two-photon applications. The recently developed model of the effect of local protein environment on 2PA (**Box 3**) should make it possible to increase the 2PA cross-section by manipulating the strength and direction of the electric field inside the barrel. New generations of mutants with even brighter two-photon fluorescence will inevitably be created. Large 2PA cross-sections and quantum yields are only part of the solution, however. In 2PLSM, the photostability of the probe is a serious constraint. To date, there is very limited information on the nonlinear multiphoton photobleaching of fluorescent proteins, and it is often difficult to compare measurements directly because the bleaching rate depends on several laser parameters in a complex way[4,32–37] and can vary dramatically between fluorescent proteins[38].

At the rather high excitation intensities usually required for 2PLSM (10^5–10^7 W cm^{-2} at the sample), the photobleaching rate rises with laser intensity more steeply than the expected quadratic function[4,32,33]. This means that lowering the peak power while raising the repetition rate can reduce total photodamage while producing the same fluorescence signal[34]. One possible explanation for the very steep power dependence of the photobleaching could be a further (stepwise) absorption from a long-lived triplet state[35]. This is consistent with the observation that lowering the repetition rate while maintaining the same peak power can be beneficial[35], although the improvement comes at the cost of longer acquisition times.

The photophysical mechanisms of nonlinear photobleaching remain unclear. The first step will be to carefully characterize the multiphoton photobleaching rates of a broad set of fluorescent proteins, which should then lead to a structure-property model that can be used to develop new variants more suitable for 2PLSM and other challenging applications. There is empirical evidence that reducing the photon energy (that is, increasing wavelength) often provides better photostability in 2PLSM. The photobleaching of DsRed slows down by an order of magnitude when the excitation wavelength is shifted to the red, from 750 to 950 nm[32]. Similarly, excitation of EGFP at 920 nm provides the twofold improvement compared to 850 nm[4], and the red protein (tdRFP) is much more stable upon 1,100-nm excitation than the green protein (EGFP) excited at 850 nm or 920 nm[4]. These observations—and the high two-photon excitation brightness near 1,050–1,150 nm of mOrange, TagRFP, tdTomato, DsRed, tdKatushka2 and mKate2—indicate that these probes can offer new opportunities for deep-tissue imaging.

Note: Supplementary information is available on the Nature Methods website.

ACKNOWLEDGMENTS

This work was supported by the US National Institute of General Medical Sciences grant R01 GM086198. We thank B.H. Davis for technical help, and R. Campbell (University of Alberta, Edmonton, Canada), D.M. Chudakov (Shemyakin and Ovchinnikov Institute of Bioorganic Chemistry, Moscow), M. Lin (Stanford University) and R.Y. Tsien (University of California San Diego) for providing us cDNA of different fluorescent proteins.

COMPETING FINANCIAL INTERESTS

The authors declare no competing financial interests.

Published online at http://www.nature.com/naturemethods/.
Reprints and permissions information is available online at http://www.nature.com/reprints/index.html.

1. Xu, C., Zipfel, W., Shear, J.B., Williams, R.M. & Webb, W.W. Multiphoton fluorescence excitation: new spectral windows for biological nonlinear microscopy. *Proc. Natl. Acad. Sci. USA* **93**, 10763–10768 (1996).
2. Zipfel, W.R., Williams, R.M. & Webb, W.W. Nonlinear magic: multiphoton microscopy in the biosciences. *Nat. Biotechnol.* **21**, 1369–1377 (2003).
3. Tsai, P.S. *et al.* All-optical histology using ultrashort laser pulses. *Neuron* **39**, 27–41 (2003).
4. Herz, J. *et al.* Expanding two-photon intravital microscopy to the infrared by means of optical parametric oscillator. *Biophys. J.* **98**, 715–723 (2010).
5. Tsien, R.Y. The green fluorescent protein. *Annu. Rev. Biochem.* **67**, 509–544 (1998).
6. Chudakov, D.M., Matz, M.V., Lukyanov, S. & Lukyanov, K.A. Fluorescent proteins and their applications in imaging living cells and tissues. *Physiol. Rev.* and references therein **90**, 1103–1163 (2010).
7. Adam, V. *et al.* Data storage based on photochromic and photoconvertible fluorescent proteins. *J. Biotechnol.* **149**, 289–298 (2010).
8. Moneron, G. & Hell, S.W. Two-photon excitation STED microscopy. *Opt. Express* **17**, 14567–14573 (2009).
9. Vaziri, A., Tang, J., Shroff, H. & Shank, C.V. Multilayer three-dimensional super resolution imaging of thick biological samples. *Proc. Natl. Acad. Sci. USA* **105**, 20221–20226 (2008).
10. Shaner, N.C., Steinbach, P.A. & Tsien, R.Y. A guide to choosing fluorescent proteins. *Nat. Methods* **2**, 905–909 (2005).
11. Drobizhev, M., Tillo, S., Makarov, N.S., Hughes, T.E. & Rebane, A. Absolute two-photon absorption spectra and two-photon brightness of orange and red fluorescent proteins. *J. Phys. Chem. B* **113**, 855–859 (2009).
12. Tillo, S.E., Hughes, T.E., Makarov, N.S., Rebane, A. & Drobizhev, M. A new approach to dual-color two-photon microscopy with fluorescent proteins. *BMC Biotechnol.* **10**, 6 (2010).
13. Makarov, N.S., Drobizhev, M. & Rebane, A. Two-photon absorption standards in the 550–1600 nm excitation wavelength range. *Opt. Express* **16**, 4029–4047 (2008).
14. Drobizhev, M., Makarov, N.S., Hughes, T. & Rebane, A. Resonance enhancement of two-photon absorption in fluorescent proteins. *J. Phys. Chem. B* **111**, 14051–14054 (2007).
15. Blab, G.A., Lommerse, P.H.M., Cognet, L., Harms, G.S. & Schmidt, T. Two-photon excitation action cross-sections of the autofluorescent proteins. *Chem. Phys. Lett.* **350**, 71–77 (2001).
16. Nifosi, R. & Luo, Y. Predictions of novel two-photon absorption bands in fluorescent proteins. *J. Phys. Chem. B* **111**, 14043–14050 (2007).
17. Nguyen, Q.T. *et al.* An *in vivo* biosensor for neurotransmitter release and *in situ* receptor activity. *Nat. Neurosci.* **13**, 127–132 (2010).
18. Kawano, H., Kogure, T., Abe, Y., Mizuno, H. & Miyawaki, A. Two-photon dual-color imaging using fluorescent proteins. *Nat. Methods* **5**, 373–374 (2008).
19. Shu, X., Shaner, N.C., Yarbrough, C.A., Tsien, R.Y. & Remington, S.J. Novel chromophores and buried charges control color in mFruits. *Biochemistry* **45**, 9639–9647 (2006).
20. Drobizhev, M., Tillo, S., Makarov, N.S., Hughes, T.E. & Rebane, A. Color hues in red fluorescent proteins are due to internal quadratic Stark effect. *J. Phys. Chem. B* **113**, 12860–12864 (2009).

21. Wachter, R.M., Elsliger, M.-A., Kallio, K., Hanson, G.T. & Remington, S.J. Structural basis of spectral shifts in the yellow-emission variants of green fluorescent protein. *Structure* **6**, 1267–1277 (1998).
22. Heikal, A.A., Hess, S.T. & Webb, W.W. Multiphoton molecular spectroscopy and excited-state dynamics of enhanced green fluorescent protein (EGFP): acid-base specificity. *Chem. Phys.* **274**, 37–45 (2001).
23. Heikal, A.A., Hess, S.T., Baird, G.S., Tsien, R.Y. & Webb, W.W. Molecular spectroscopy and dynamics of intrinsically fluorescent proteins: coral red (dsRed) and yellow (Citrine). *Proc. Natl. Acad. Sci. USA* **97**, 11996–12001 (2000).
24. Hashimoto, H. *et al.* Measurement of two-photon excitation spectra of fluorescent proteins with nonlinear Fourier-transform spectroscopy. *Appl. Opt.* **49**, 3323–3329 (2010).
25. Piatkevich, K.D. *et al.* Monomeric red fluorescent proteins with a large Stokes shift. *Proc. Natl. Acad. Sci. USA* **107**, 5369–5374 (2010).
26. Rizzo, M.A., Springer, G., Segawa, K., Zipfel, W.R. & Piston, D.W. Optimization of pairings and detection conditions for measurements of FRET between cyan and yellow fluorescent proteins. *Microsc. Microanal.* **12**, 238–254 (2006).
27. Hosoi, H., Yamaguchi, S., Mizuno, H., Miyawaki, A. & Tahara, T. Hidden electronic excited state of enhanced green fluorescent protein. *J. Phys. Chem. B* **112**, 2761–2763 (2008).
28. Oulianov, D.A., Tomov, I.V., Dvornikov, A.S. & Rentzepis, P.M. Observations on the measurement of two-photon absorption cross-section. *Opt. Commun.* **191**, 235–243 (2001).
29. Albota, M.A., Xu, C. & Webb, W.W. Two-photon fluorescence excitation cross sections of biomolecular probes from 690 to 960 nm. *Appl. Opt.* **37**, 7352–7356 (1998).
30. Kredel, S. *et al.* Optimized and far-red-emitting variants of fluorescent protein eqFP611. *Chem. Biol.* **15**, 224–233 (2008).
31. Shaner, N.C. *et al.* Improved monomeric red, orange and yellow fluorescent proteins derived from *Discosoma* sp. red fluorescent protein. *Nat. Biotechnol.* **22**, 1567–1572 (2004).
32. Marchant, J.S., Stutzmann, G.E., Leissring, M.A., LaFerla, F.M. & Parker, I. Multiphoton-evoked color change of DsRed as an optical highlighter for cellular and subcellular labeling. *Nat. Biotechnol.* **19**, 645–649 (2001).
33. Chen, T.-S., Zeng, S.-Q., Luo, Q.-M., Zhang, Z.-H. & Zhou, W. High-order photobleaching of green fluorescent protein inside live cells in two-photon excitation microscopy. *Biochem. Biophys. Res. Commun.* **291**, 1272–1275 (2002).
34. Ji, N., Magee, J.C. & Betzig, E. High-speed, low-photodamage nonlinear imaging using passive pulse splitters. *Nat. Methods* **5**, 197–202 (2008).
35. Donnert, G., Eggeling, C. & Hell, S.W. Major signal increase in fluorescence microscopy through dark-state relaxation. *Nat. Methods* **4**, 81–86 (2007).
36. Kawano, H. *et al.* Attenuation of photobleaching in two-photon excitation fluorescence from green fluorescent protein with shaped excitation pulses. *Biochem. Biophys. Res. Commun.* **311**, 592–596 (2003).
37. Field, J.J. *et al.* Optimizing the fluorescent yield in two-photon laser scanning microscopy with dispersion compensation. *Opt. Express* **18**, 13661–13672 (2010).
38. Patterson, G.H., Knobel, S.M., Sharif, W.D., Kain, S.R. & Piston, D.W. Use of the green fluorescent protein and its mutants in quantitative fluorescence microscopy. *Biophys. J.* **73**, 2782–2790 (1997).
39. Ritz, J.-P. *et al.* Optical properties of native and coagulated porcine liver tissue between 400 and 2400 nm. *Lasers Surg. Med.* **29**, 205–212 (2001).
40. Ai, H.W., Shaner, N.C., Cheng, Z., Tsien, R.Y. & Campbell, R.E. Exploration of new chromophore structures leads to the identification of improved blue fluorescent proteins. *Biochemistry* **46**, 5904–5910 (2007).
41. Rizzo, M.A., Springer, G.H., Granada, B. & Piston, D.W. An improved cyan fluorescent protein variant useful for FRET. *Nat. Biotechnol.* **22**, 445–449 (2004).
42. Ai, H.W., Henderson, J.N., Remington, S.J. & Campbell, R.E. Directed evolution of a monomeric, bright and photostable version of *Clavularia* cyan fluorescent protein: structural characterization and applications in fluorescence imaging. *Biochem. J.* **400**, 531–540 (2006).
43. Ai, H.W., Hazelwood, K.L., Davidson, M.W. & Campbell, R.E. Fluorescent protein FRET pairs for ratiometric imaging of dual biosensors. *Nat. Methods* **5**, 401–403 (2008).
44. Griesbeck, O., Baird, G.S., Campbell, R.E., Zacharias, D.A. & Tsien, R.Y. Reducing the environmental sensitivity of yellow fluorescent protein. *J. Biol. Chem.* **31**, 29188–29194 (2001).
45. Tsutsui, H., Karasawa, S., Okamura, Y. & Miyawaki, A. Improving membrane voltage measurements using FRET with new fluorescent proteins. *Nat. Methods* **5**, 683–685 (2008).
46. Merzlyak, E.M. *et al.* Bright monomeric red fluorescent protein with an extended fluorescence lifetime. *Nat. Methods* **4**, 555–557 (2007).
47. Yanushevich, Y.G. *et al.* A strategy for the generation of non-aggregating mutants of *Anthozoa* fluorescent proteins. *FEBS Lett.* **511**, 11–14 (2002).
48. Wang, L., Jackson, W.C., Steinbach, P.A. & Tsien, R.Y. Evolution of new nonantibody proteins via iterative somatic hypermutation. *Proc. Natl. Acad. Sci. USA* **101**, 16745–16749 (2004).
49. Shcherbo, D. *et al.* Far-red fluorescent tags for protein imaging in living tissues. *Biochem. J.* **418**, 567–574 (2009).
50. Lin, M.Z. *et al.* Autofluorescent proteins with excitation in the optical window for intravital imaging in mammals. *Chem. Biol.* **16**, 1169–1179 (2009).